Hindawi
Adsorption Science & Technology
Volume 2021, Article ID 6629365, 18 pages
https://doi.org/10.1155/2021/6629365

Research Article

CO_2 Adsorption Capacity of Organic Alkali Sorbent CPEI from Polyethyleneimine

Feng Wang, Lu Yu, Youhua Li, and Dengfa Huang

School of Chemical and Material Engineering, Jiangnan University, Wuxi 214122, China

Correspondence should be addressed to Feng Wang; fwang@jiangnan.edu.cn

Received 17 September 2020; Accepted 18 December 2020; Published 19 January 2021

Academic Editor: Ashleigh Fletcher

Support-free cross-linked polyethyleneimine sorbent (CPEI) for CO_2 capture was evaluated as the regenerable sorbent. The total amines available for the CO_2 capture on CPEI were determined by the polyethyleneimine/glutaraldehyde ratio for the synthesis of CPEI. The CO_2 capacity of CPEI in the slurry bubble column reactor reached 4.92 mmol/g, which is 1.97 times higher than that obtained under anhydrous conditions. The adsorption kinetics of CPEI in the reactor were investigated in terms of the CPEI amount, the CO_2 fraction, the gas flow rate, temperature, and the total amines available. The experimental breakthrough curves for the sorbent were well-fitted with a fractional-order kinetic model. The modeling analysis found the influence of diffusion resistance on the adsorption is more significant than that of the driving force. The CO_2 capacity of CPEI remained almost constant during the temperature swing adsorption/desorption cycles.

1. Introduction

Anthropogenic activity is the main cause of the increased atmospheric concentrations of CO_2 [1]. The long-term exposure to the CO_2 level higher than 0.5% can cause severe health problems, such as fatigue, listlessness, malaise, mood changes, and headache [2–4]. Hence, the removal of CO_2 from cabin atmosphere is a critical function of the life support system of submarine and space capsule [5].

The removal of CO_2 from the ambient environment can be achieved by applying a variety of physical and chemical processes such as aqueous solutions of alkanolamine absorption [6], membrane separation [7], and biological capture [8]. Chemical absorption/adsorption is regarded as one of the most promising CO_2 capture technologies. It has been widely used due to its high efficiency, low energy consumption, environmental friendliness, etc. [9, 10].

Amine can react with CO_2 to form ammonium carbamates and carbonates reversibly at moderate temperature [11]. Chemical absorption using liquid amine has been commercially used in large-scale CO_2 capture [12]. However, there are issues of corrosion and degradation in the applications of liquid amines for CO_2 capture [13]. Besides, the solution state of CO_2 capture makes the endothermic regeneration step (stripping) energy-intensive and costly [14].

Solid adsorbents are promising candidates for reduced regeneration energy, greater capacity, minimized corrosion issue, selectivity, ease of handling, etc. [15]. Amine-based solid sorbents are a group of materials or supports modified physically or chemically with amine groups for CO_2 uptake in open and closed environments [16–19]. Amine-based solid sorbents can be obtained by (1) impregnating amines into the pores of support, (2) chemically binding amines to support, known as grafting, and (3) polymerizing amine monomers in situ, resulting in polyamine structures tethered to the walls of support [20, 21]. Such hybrid amine-modified sorbents have been used successfully onboard the space vehicles for crew air scrubbing [22].

Among various amine-based solid sorbents, polyethyleneimine- (PEI-) impregnated supports like mesoporous silicas and mesoporous molecular sieve and resin have attracted extensive attention because of their high CO_2 adsorption capacity, easy availability, and stability [23–26]. The loading of amines onto the outer and interior surfaces

of the supports by impregnation is simple and has been extensively studied [27, 28]. However, the physically impregnated PEI on support is structurally unstable and detachment from the support occurred easily in the absence of chemical bonds [29]. Amine-grafted sorbents exhibit more stability over many cycles owing to the formation of covalent bonds between the support surface and amines [30, 31]. However, the covalent tethering of PEI on the support is limited by the surface area, the number of accessible active groups [32]. The solid CO_2 adsorbents may be further improved by eliminating the use of inert supports. Wang et al. prepared a support-free polyamine porous particle by cross-linking N-methyl-N-vinylformamide with di[2-(N-vinylformamido)ethyl] [33]. The CO_2 capture capacity of the sorbent reached 2.3 mmol/g. Yoo et al. obtained a self-supported, branched poly(ethyleneimine) material with poly(ethylene glycol) diglycidyl ether as the cross-linker via an ice templating method [34]. The CO_2 uptake of the material reached 5.5 mol CO_2 per kg sorbent at 65% relative humidity. Other cross-linkers, such as glutaraldehyde [35] and diglycidyl ether [36], have also been applied for the cross-linking of polyethyleneimine (PEI) to synthesize support-free CO_2 sorbent materials. The CO_2 capacity of the support-free sorbent formed by the cross-linking PEI with diglycidyl ether displays a CO_2 uptake of 4.43 mmol CO_2/g (90°C) under anhydrous conditions and 5.34 mmol/g in the presence of humidity. A slurry bubble column reactor (SBCR) is frequently used where heterogeneous gas-liquid and gas-solid-liquid operations and reactions take place [2]. The reactor has been applied in CO_2 capture using magnesium hydroxide or calcium hydroxide particles as sorbents [37–39]. In the SBCR, the gas is dispersed in the liquid and/or solid phases in the shape of bubbles, which provides high contact areas. Furthermore, the small particles in the slurry can improve the surface renewal and turbulence in the liquid film at the gas-liquid interface increasing mass transfer coefficients [40]. The presence of fine particles in the liquid film can also hinder the coalescence behavior of bubbles, consequently increasing the gas-liquid interfacial area [40]. In the literature, the evaluation of CO_2 capture on solid sorbents by a fixed bed system was often reported [41, 42]. The high particle attrition rate and the pressure drop built up in the fixed bed increase the blower power required to maintain flow and eventually require highly undesirable system maintenance [43].

In the present study, support-free cross-linked polyethyleneimine microspheres (CPEI) was proposed as the regenerable sorbent for CO_2 capture. The CPEI is abundant in amino groups by avoiding the use of inert support as in the cases of amine-modified sorbents. The CO_2 capacity of CPEI was evaluated by the thermogravimetric analysis (TGA) method and the SBCR method using mixing gases of CO_2 and N_2.

2. Materials and Methods

2.1. Materials. Polyethyleneimine (Mw = 70000 Da, 50% aqueous solution), liquid paraffin (≥99.7%), Span-80 (chemically pure), Tween-80 (chemically pure), and glutaraldehyde solution (25 wt %) were purchased from Sinopharm Chemical Reagent Co., Ltd. (Shanghai, China). Pure CO_2 gas (>99%) and pure N_2 gas (>99%) were purchased from Wuxi Xinxiyi Technology Co., Ltd., China. The other reagents are used as received without further purification.

2.2. Synthesis of CPEI. In a 25 ml stoppered vial (27 × 72 mm), 7 ml of 20wt % PEI aqueous solution (pH = 2, adjusted with 12 mol/l HCl), 0.15 g Tween-80, and a certain amount of glutaraldehyde (GA, 25 wt %) were mixed. After the addition of 12 ml liquid paraffin solution of 0.7 g Span-80, the mixture was homogenized at 6000 rpm for 3 min at 20°C. Thereafter, 4 ml of 1.0 mol/l NaOH solution was added dropwise into the mixture at a speed of 2 ml/min. The reaction was carried out 4.5 h at 20°C under magnetic stirring (150 rpm). CPEI was obtained by centrifugation at 15000 rpm for 5 min. The sorbents were washed several times with absolute ethanol and anhydrous diethyl ether and dried under vacuum at room temperature. The influence of various PEI/GA ratio on the properties of CPEI was estimated at 2 : 1, 4 : 1, and 7 : 1 (g : g).

2.3. CO_2 Adsorption Capacity of CPEI by the SBCR Method. Scheme 1 shows the experimental setup for CO_2 capture using an SBCR as the mass transfer device. It consisted of a cylindrical vessel (120 cm high and 5 cm inner diameter) and a gas sparger at the bottom. The working volume of the reactor was 25 ml. The gas sparger installed in the middle of the bottom of the column was a stainless steel 316 l porous metal micro sparger with a pore size of 15 μm (Mott Corporation, U.S.). The gas was made by mixing pure CO_2 gas with pure N_2 gas at 101.3 kPa and 25°C. The flow rates of the two gas streams were controlled by mass flow controllers (thermal gas mass flow controller, Cole-Parmer Inc.; range: 0-5 l/min, accuracy: ±0.5% of full scale). The sorbents sat in the column. The temperature was set to the adsorption temperature to be evaluated. The mixed gas was then passed into the reactor. The influent and effluent gas streams flowed into a gas chromatograph (GC) equipped with a thermal conductivity detector (TCD) by an autosampling system. All operation pressure is atmospheric pressure. Before each run, the sorbents in the reactor drained of liquid were regenerated by purging with N_2 at 100°C until no CO_2 or water was detected in the exhaust gas.

The CO_2 uptake capacity curves for CPEI were calculated by integrating the breakthrough curves according to Equation (1) where q_t is the adsorption capacity of slurry (mmol/ml) at time t, s is the flow rate of the feed gas (mmol/min), v is the volume of slurry in the bed (ml), v_d is the voids of the reactor (ml), and t is the adsorption time (min). p is the pressure of the reactor (Pa). T is the temperature of the slurry (K). C_0 and C_t are the CO_2 concentrations (mol/mol) in the feed gas and the exhaust gas at time t, respectively. Q_t in Equation (2) is the adsorption capacity of CPEI (mmol/g) at time t. m is the sorbent fraction in the slurry (g/ml). q_0 is the adsorption capacity (mmol/ml) of blank water of slurry.

$$q_t = \int_0^t \left[\frac{s}{v} \left(C_0 - \frac{1 - C_0}{1 - C_t} C_t \right) - \frac{44 \times 10^3 p}{8.314 T} \times \frac{v_d C_t}{v} \right] dt, \quad (1)$$

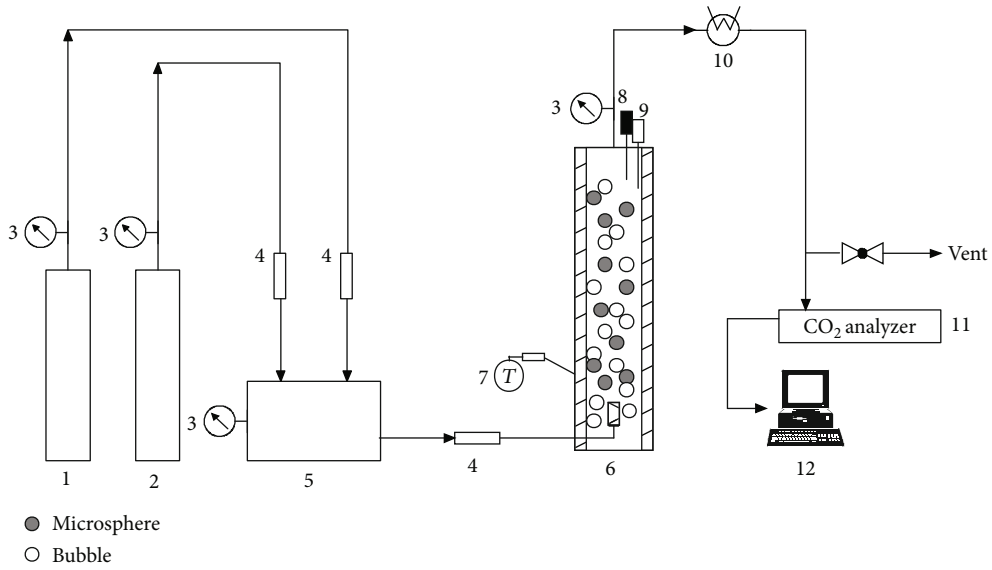

Scheme 1: Schematic diagram of the experimental setup of the SBCR (1) N_2 cylinder, (2) CO_2 cylinder, (3) pressure gauge, (4) gas flow controller, (5) gas mixer, (6) slurry bubble column, (7) temperature controller, (8) pH probe, (9) thermocouple, (10) condenser, (11) CO_2 analyzer, and (12) computer.

$$Q_t = (q_t - q_0) \times m. \tag{2}$$

2.4. Kinetic Model. The fractional-order kinetic model (Equation (3)) proposed by Heydari-Gorji and Sayari has been proved to be suitable for describing the CO_2 adsorption on amine-modified sorbents [5, 44]. The fractional-order kinetic model represents the complexity of the reaction mechanism that may involve more than one reaction pathway [45]. In this model, the adsorption rate is proportional to the nth power of the driving force and the mth power of the adsorption time:

$$\frac{1}{q_e - q_t} = \left[\left(\frac{(n-1)k_n}{m}\right)t^m + \frac{1}{q_e^{n-1}}\right]^{1/(n-1)}, \tag{3}$$

where q_e and q_t are the sorption capacity at adsorption equilibrium and at time t; k_n, n, and m are the model constants. k_n is regarded as the adsorption rate constant of the kinetic model. The value of n reflects the pseudo-order of reaction with respect to the driving force. For $n = 1$, Equation (3) turns to the Avrami equation; for $m = 1$ and $n = 1$ or 2, Equation (3) turns to the pseudo-first-order or pseudo-second-order kinetic model, respectively [44].

The parameters of the fractional-order kinetic model (Equation (3)) were obtained by regression analysis of the experimental data of this work using the Levenberg-Marquardt optimization algorithm in the MATLAB toolbox.

2.5. CO_2 Adsorption Capacity of CPEI under Anhydrous Conditions. A thermogravimetric analyzer (Mettler-Toledo International Inc., Zürich, Switzerland) was used to assess the CO_2 capacity as a function of time. In a typical adsorption run, about 10 mg of the sorbent was placed in a platinum pan. 100% CO_2 gas was used for the adsorption measurements at 101.3 kPa. To drive off the preadsorbed gases, moisture, or any other impurities, CPEI was first degassed at 100°C for about 20 min with N_2 at the flow rate of 100 ml/min. Then, the temperature was decreased to the desired adsorption temperature. CO_2 capture measurements were carried out by exposing the samples to CO_2 with a flow rate of 100 ml/min.

In order to test the reversibility and stability of CPEI, repeated adsorption/desorption operations were performed for 20 cycles to examine the regeneration characteristics of each sample. Regeneration of sorbent was carried out on the same experimental TGA setup. The saturated sorbent of CO_2 was purged with purified N_2 gas stream at 100°C for about 20 min in order to be generated for the next cycle step.

2.6. Characterization. Fourier transformation infrared spectra (FT-IR) were obtained using a Tensor 27 spectrometer (Bruker Corporation, Ettlingen, Germany). Thermogravimetry analysis (TGA) was performed on a TGA/SDTA851e thermogravimetric analyzer (Mettler-Toledo International Inc., Zürich, Switzerland). The morphological structure of CPEI was examined by an S-4800 scanning electron microscope (Hitachi Ltd., Tokyo, Japan). The diameter distribution of CPEI was determined by the method described by Cohen et al. [46]. A 2,2′-bicinchoninic acid (BCA) assay method was used to determine the quantity of the primary and secondary amine group of the sorbent [47]. The tertiary amino groups were determined by titration with perchloric acid [48]. The nitrogen sorption isotherms of CPEI at 77 K were determined by a Micromeritics 3Flex surface characterization analyzer (USA). Before the measurement, the microspheres were degassed at 373 K for 12 hours. The BET surface area and pore volume were determined by Brunauer-Emmett-Teller (BET) and Barrett-Joyner-Halenda (BJH) methods.

3. Results and Discussion

3.1. Characterization of CPEI. The CPEI sorbents were synthesized in 12 ml liquid paraffin solution under the conditions of 0.7 g Span-8, 7 ml of 20 wt % PEI solution, 0.15 g Tween-80, and GA (25 wt %) with homogenization at 6000 rpm for 3 min at 20°C. Three types of CPEI, CPEI-1, CPEI-2, and CPEI-3, were obtained at the PEI/GA ratio of 2 : 1, 4 : 1, and 7 : 1 (g : g), respectively. Images of CPEI obtained by scanning electron microscopy (SEM) are displayed in Figure 1. The microsphere of CPEI is regular in shape with a PDI value (the polydispersity index) of 1.04. The diameter distribution of the sorbents was in the range of 1.42-4.45 μm.

FT-IR spectra of CPEI-1, CPEI-2, and CPEI-3 were found to be similar. Using as an instance, the spectrum of CPEI-3 is displayed in Figure 2. The characteristic peaks are at 3534-3422 cm^{-1} (-N-H stretching), 2930-2855 cm^{-1} (-C-H stretching), 1653 cm^{-1} (-C=N stretching), 1569 cm^{-1} (-N-H in-plane bending), 1446 cm^{-1} (-C-H bending), 1341-1031 cm^{-1} (-C-N stretching), and 944 cm^{-1} (-N-H out-of-plane bending). With CO_2 adsorbed on CPEI, the peak at 1569 cm^{-1} can also be assigned to the N-H deformation in carbamates [49].

According to Figure 3, CPEI-1, CPEI-2, and CPEI-3 showed two common weight losses in the 150-500°C range, with total weight losses of 91%. The two-stage weight loss was accomplished when samples were heated to 278°C and 475°C, respectively. In the first weight-loss event, the sorbent lost 5% of its weight, due to the released CO_2 and other small molecules. The CO_2 released is previously adsorbed by CPEI from ambient air. In the second stage of weight loss, the total weight loss in 278-475°C was about 85% of the initial weight owing to the decomposition of the sorbent. It can be also found that CPEI decomposed faster with an increasing ratio of PEI/GA (Figure 3).

Glutaraldehyde (GA), epichlorohydrin, N-hydroxysuccinimide esters, and imidoesters have been used to cross-link polymers such as chitosan and protein, through Schiff reactions with amino groups [50]. GA has the advantages of commercial availability, low cost, and high reactivity. Excess glutaraldehyde waste after reaction can be easily detoxified by mixing with glycine [51]. Thus, GA was used in this work to cross-link PEI through emulsion cross-linking polymerization for obtaining CPEI sorbents. According to the results displayed in Table 1, an increase of the value of total amines of CPEI was observed when the PEI/GA ratio used for the synthesis of CPEI increased from 2 : 1 to 7 : 1 (g : g). The further increase of the PEI/GA ratio resulted in the collapsed or broken microsphere (Figure S1). This may be due to the decrease in the strength of the microsphere wall formed by reducing the amount of the cross-linker GA. Therefore, the following studies were conducted with the CPEI sorbents obtained at the PEI/GA ratio of 2 : 1, 4 : 1, and 7 : 1.

According to the data listed in Table 1, the fraction of primary and secondary amines of CPEI increased with the increase of the PEI/GA ratio used for the synthesis of sorbent. The triple ratio of primary amines to secondary amines to tertiary amines (mol : mol : mol) increased from 3.74 : 2.59 : 1 (CPEI-1) and 3.86 : 2.61 : 1 (CPEI-2) to 4.36 : 3.02 : 1 (CPEI-3). Primary amines and secondary amines react rapidly with CO_2 to form carbamates (Equations (4) and (5)). According to the mechanism proposed by Caplow [52], the reaction between CO_2 and the primary and secondary amine involves the formation of a zwitterion and the deprotonation of the zwitterion by a basic amine, resulting in the formation of carbamate:

$$CO_2 + 2RNH_2 \rightleftharpoons RNHCOO^- + RNH_3^+ \quad (4)$$

$$CO_2 + 2R_2NH \rightleftharpoons R_2NCOO^- + R_2NH_2^+ \quad (5)$$

The zwitterion can react easily with water via the formation of bicarbonates [18, 53, 54]. In this case, only one amino group is necessary for reaction with one CO_2 molecule (Equations (6) and (7)) instead of two in the case of carbamate formation under the anhydrous conditions (Equations (4) and (5)).

$$CO_2 + RNH_2 + H_2O \rightleftharpoons RNH_3^+ + HCO_3^- \quad (6)$$

$$CO_2 + R_2NH + H_2O \rightleftharpoons R_2NH_2^+ + HCO_3^- \quad (7)$$

Tertiary amines are hindered amines which possess no hydrogen atom attached to the nitrogen atom, as in the case of primary and secondary amines. Thus, tertiary amines do not react directly with carbon dioxide [55]. Instead, tertiary amines facilitate the CO_2 hydrolysis reaction forming bicarbonates (Equation (8)) [55]. A base-catalysis reaction mechanism involving a very instable zwitterion was suggested by Yu et al. for tertiary amines [56].

$$CO_2 + R_3N + H_2O \rightleftharpoons R_3NH^+ + HCO_3^- \quad (8)$$

Recently, the use of mixed amine absorbents, such as blends of primary and tertiary amines or secondary and tertiary amines, aroused great interest, due to the combination of the higher equilibrium capacity of the tertiary amine with the higher reaction rate of primary or secondary amine [57]. In order to achieve both fast absorption rates and low regeneration energy consumption, the sorbents such as CPEI of mixed amines becomes more and more attractive [58].

Figure 4 displays the typical N_2 adsorption/desorption isotherms of CPEI prepared at the PEI/GA ratio (g : g) of 2 : 1 (a), 4 : 1 (b), and 7 : 1 (c), respectively. As seen from Figure 4, CPEI sorbents show typical type III isotherm. The BET surface area of CPEI sorbent is 7.44, 5.63, and 4.19 m^2/g at the PEI/GA ratio of 2 : 1, 4 : 1, and 7 : 1 (g : g), respectively. Correspondingly, the pore volume was determined as 0.022 cm^3/g (2 : 1), 0.004 cm^3/g (4 : 1), and 0.022 cm^3/g (7 : 1), respectively.

3.2. CO_2 Capacity of CPEI under Anhydrous Conditions. Thermogravimetric analysis is the common approach used in the literature for determining the CO_2 capacity of sorbent under anhydrous conditions [18]. Herein, the CO_2 capacity of CPEI-1, CPEI-2, and CPEI-3 was measured at 50°C in the pure CO_2 stream by the TGA method, respectively, and

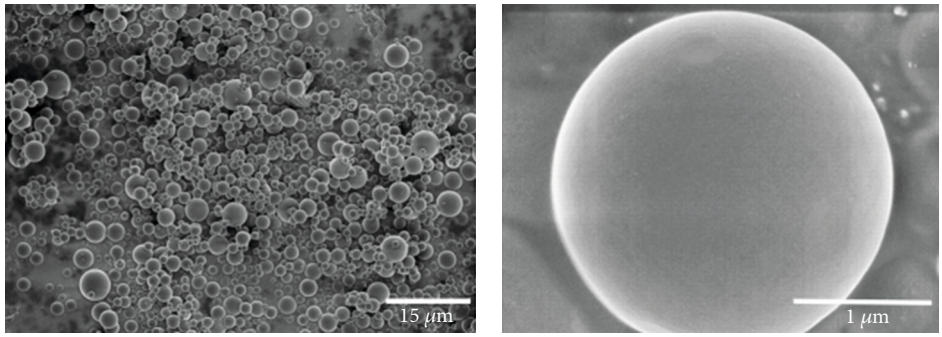

Figure 1: SEM images of CPEI (a) microsphere aggregates; (b) zoom-in image of an intact microsphere.

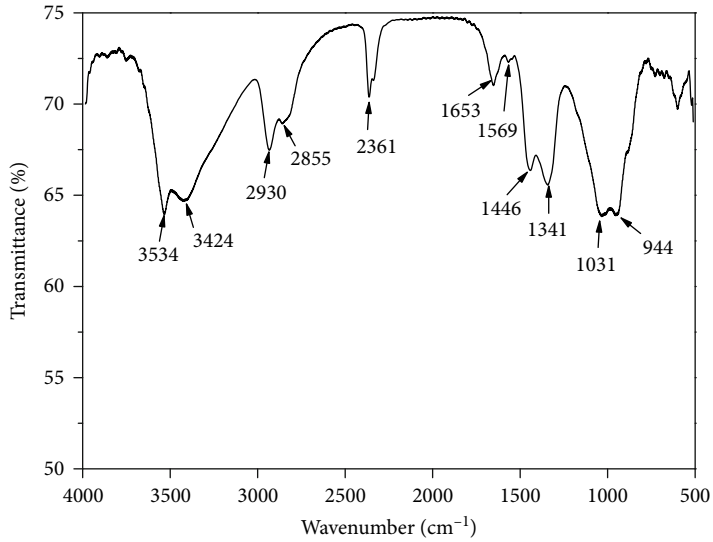

Figure 2: FT-IR spectrum of CPEI-3.

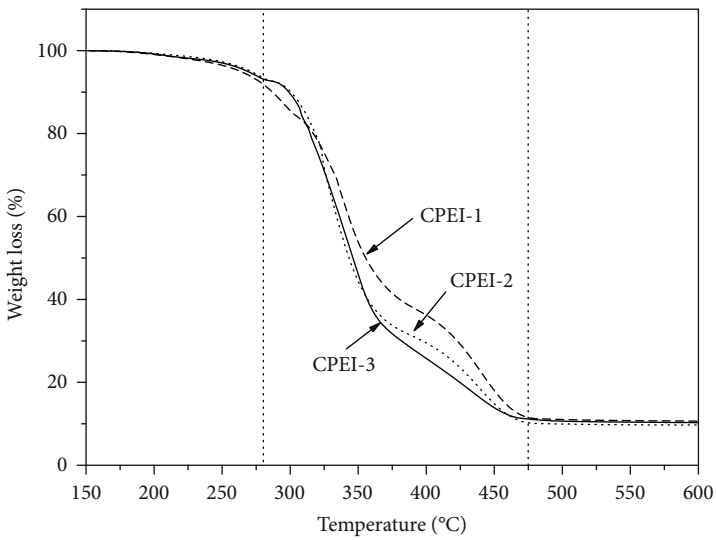

Figure 3: TGA curves of CPEI-1, CPEI-2, and CPEI-3.

Table 1: Influences of various PEI/GA ratios used for the synthesis of CPEI on the total amine, primary amine, secondary amine, and tertiary amine values of CPEI.

	CPEI sorbents		
	CPEI-1	CPEI-2	CPEI-3
PEI/GA ratio (g : g)	2 : 1	4 : 1	7 : 1
Total amines (mmol/g)	6.74 ± 0.12	7.18 ± 0.15	7.63 ± 0.13
Primary amines (mmol/g)	3.44 ± 0.06	3.71 ± 0.08	3.97 ± 0.07
Secondary amines (mmol/g)	2.38 ± 0.04	2.51 ± 0.04	2.75 ± 0.03
Tertiary amines (mmol/g)	0.92 ± 0.02	0.96 ± 0.03	0.91 ± 0.03

the results are shown in Figure 5. The CO_2 capacities rise and flatten out in 60 min from the start of adsorption. With the increase of the PEI/GA ratio, the equilibrium CO_2 capacity on CPEI sorbents increases and reaches the maximal capacity using CPEI-3. According to the results listed in Table 1, the value of total amines of CPEI-3 is the highest among CPEIs tested, which may account for the highest CO_2 capacity on CPEI-3.

Adsorption temperature is a momentous factor for CO_2 adsorption kinetics. The CO_2 capture curves of CPEI-3 plotted at different isothermal conditions (30, 40, 50, 60, and 70°C) are presented in Figure 6. It shows that the CO_2 capacity of the sorbent increased with the increase of adsorption temperature, reaching about 2.5 mmol/g at 50°C. A sharp decrease in the CO_2 capacity was observed when the adsorption temperature was higher than 50°C. Based on the mechanism proposed by Song's group [59], the CO_2 adsorption in the cross-linked PEI matrix of CPEI-3 may occur in two stages: the rapid sorption by amines in the exposed outer layer, followed by the diffusion of CO_2 into the microsphere to react the interior amines. At low temperature, the interior amines may not be accessible due to diffusion limitation. As the adsorption temperature was increased, the diffusion of CO_2 in the cross-linked PEI matrix was improved. The interior amines would be accessible to the CO_2, resulting in improved CO_2 capacity. However, as the adsorption temperature was increased to be higher than 50°C, the CO_2 capacity reduced sharply because the enhancement of the exothermic effect of the reaction between CO_2 and amines caused the adsorption equilibrium to shift to desorption, resulting in the decrease of CO_2 capacity [60]. A similar result was also reported by Xu et al., Chen et al., and Monazam et al. using the amine-modified sorbents [61–63].

3.3. CO_2 Capacity of CPEI Sorbents in an SBCR. A slurry bubble column reactor (SBCR) has been used in CO_2 removal utilizing fine particles such as magnesium hydroxide or calcium hydroxide as sorbents [37, 39]. In this work, the application of regenerable CPEI in the SBCR system was evaluated for CO_2 capture.

The CO_2 capacities of CPEI-1, CPEI-2, and CPEI-3 were assayed under the conditions of 0.025 g/ml CPEI, 5 mol % CO_2/N_2, and 100 ml/min gas flow rate at 20°C (Figures 7(a) and 7(b)). The CO_2 capacity elevated with the increase of the total amine value of CPEI (Table 1). Besides, the lesser cross-linked materials using less cross-linker are more permeable to CO_2, therefore allowing more amines to react with CO_2 [36]. According to Figure 5, the highest value of the CO_2 capacity of CPEI is achieved using CPEI-3.

The influence of change of adsorption temperature (from 20°C to 50°C) on the CO_2 capacity of CPEI-3 is shown in Figures 7(c) and 7(d). The CO_2 capacity reached the maximal value at 30°C under the conditions of 0.025 g/ml CPEI-3 fraction, 5 mol % CO_2/N_2, and 100 ml/min the gas flow rate under 101.3 kPa. When the temperature was increased higher than 30°C, the CO_2 capacity reduced. This may be owing to the negative impact of high temperature on the exothermic reaction of adsorption.

The investigation of the influences of various CO_2/N_2 mixtures (from 2.5 to 15 mol %) on the CO_2 capacity of CPEI-3 was conducted at 0.025 g/ml of the sorbent fraction, 100 ml/min the gas flow rate and at 20°C and 101.3 kPa. The results depicted in Figures 7(e) and 7(f) show the adsorption leveled off in a shorter time when the ratio of CO_2 to N_2 in flow increased. That is due to enhanced driving force promoting the diffusion rate of CO_2 through the increase of CO_2 concentration difference between the gas flow and the slurry. It was also found the CO_2 capacity was increased slightly, by around 9.8%, when the CO_2 fraction in N_2 was increased sixfold (from 2.5 to 15 mol %). That implies the CPEI sorbent had almost reached its adsorption saturation at 2.5 mol % of CO_2/N_2.

Figure 8 shows the influences of different CPEI-3 fractions and various gas flow rates of CO_2/N_2 mixture on the CO_2 capture of an SBCR. After introducing the flow to the SBCR, fast adsorptions of CO_2 were observed. Thereafter, the sorbent gradually got saturated and a rise in the CO_2 concentration in the outlet gas was detected until complete saturation. Figure 8(b) displays the increase of CPEI-3 fraction in the slurry resulted in the increased CO_2 capacity but prolonged the time when the CO_2 capacity plateaued. The CO_2 capacity reached the maximal value as the CPEI-3 fraction was 0.05 g/ml. The further increase of CPEI-3 fraction resulted in the reduced capacity. That is due to the increased viscosity of the slurry which has negative influences on the diffusion of CO_2 in the slurry reducing the capacity of CPEI-3 [64].

The influences of the gas flow rate on the CO_2 capture in the SBCR were investigated under the conditions of 5 mol % CO_2/N_2 mixture, 0.025 g/ml of CPEI-3 fraction at 20°C and 101.3 kPa. According to the results demonstrated in Figures 8(c) and 8(d), with the increase of the gas flow rate, the time for the CO_2 capacity to reach the equilibrium decreased. That is because the slurry is agitated more severely with the increase of gas flow rate, promoting the diffusion and the dissolution of CO_2 in the slurry [19]. However, when the gas flow rate is higher than a certain critical value, 150 ml/min in this study, the CO_2 capacity reduced due to the insufficient contact between the slurry and CO_2 at the too rapid gas flow rate.

Above all, the highest CO_2 capacity can be obtained with CPEI-3 as the sorbent in the SBCR under the conditions of

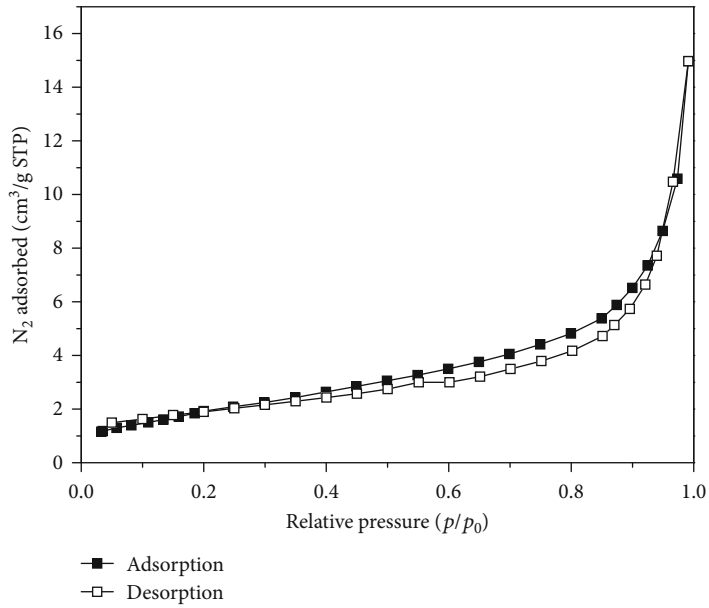

(a)

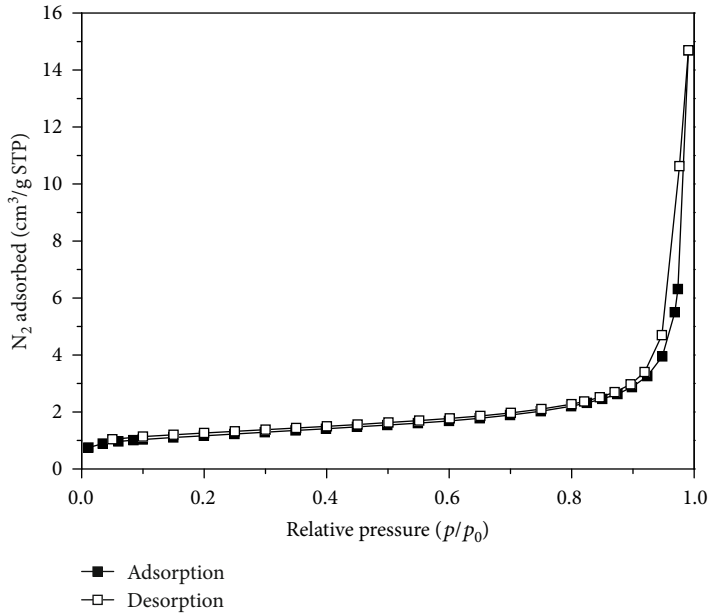

(b)

Figure 4: Continued.

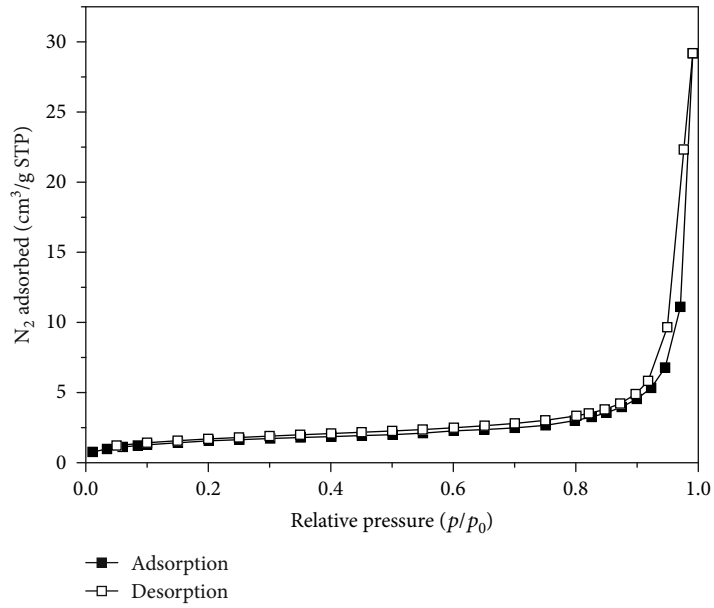

(c)

Figure 4: N_2 adsorption-desorption isotherms of CPEI-1 (a), CPEI-2 (b), and CPEI-3 (c).

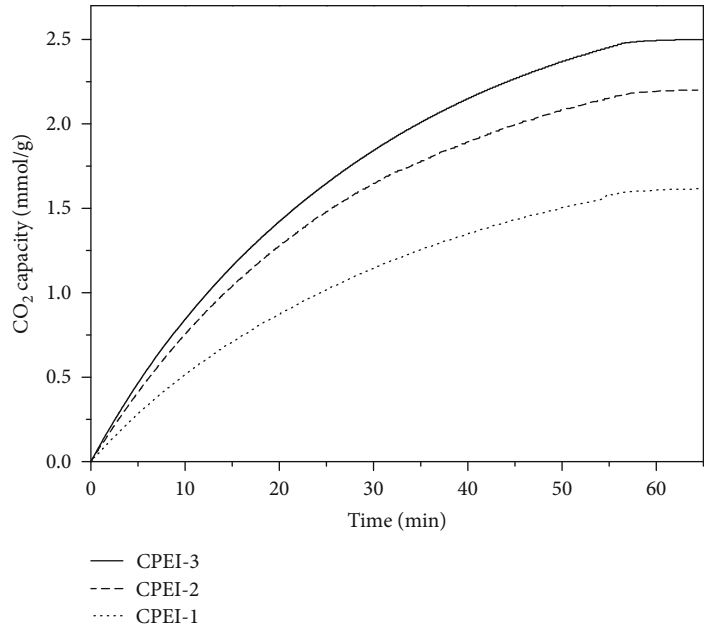

Figure 5: CO_2 capacity of CPEI-1, CPEI-2, and CPEI-3 at 80°C and 101.3 kPa.

0.05 g/ml of the sorbent fraction, 15 mol % of CO_2/N_2, 100 ml. The CO_2 capacity of CPEI sorbent determined by the TGA method is obviously lower than that obtained in the SBCR. That depends on the presence or absence of water in the two adsorption methods. Yoo et al. [34] and Hamdy et al. also found the CO_2 capacity of poly(ethylene glycol)-diglycidyl-ether-cross-linked poly(ethyleneimine) materials and diglycidyl-ether-cross-linked polyethyleneimine materials were increased by 1.95 times [34] and 1.2 times [36] in the presence of water, respectively. According to Equations (3)–(5), the presence of water can theoretically double the CO_2 capacity due to the formation of bicarbonates during the chemical interaction between the amines and CO_2. Therefore, the CO_2 capacity of the CPEI sorbent determined by the SBCR method is higher than that by the TGA method. The enhancements in the presence of water observed for CPEI sorbents were within the theoretical limit.

3.4. Kinetic Modeling Analysis. The kinetic of adsorption is important to assess the performance of adsorbents for CO_2

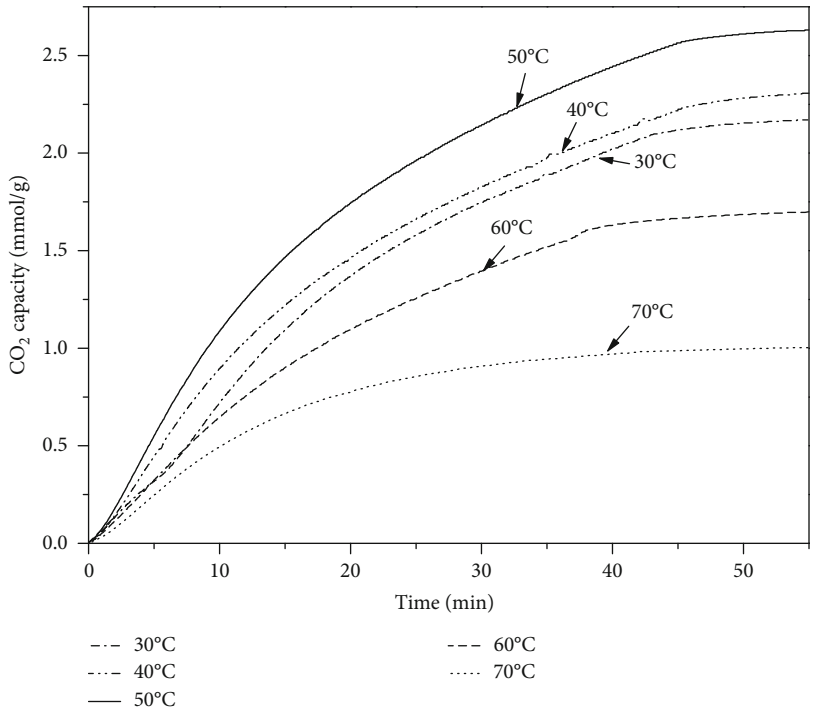

Figure 6: CO_2 capacity of CPEI-3 at different temperatures at 101.3 kPa.

removal [21]. To date, the literature provides a number of kinetic models describing the kinetics of the solute adsorption at the solid/solution interface. Several studies have been conducted on the kinetics of CO_2 adsorption on sorbents [44]. The fractional-order kinetic model (Equation (3)) developed by Heydari-Gorji et al. [44] demonstrated that two kinds of physical and chemical adsorption took place and was used to fit the data of the CO_2 adsorption on amine-modified sorbents [65]. In this work, this model was used to describe the CO_2 adsorption on CPEI-3 (Figures 7(b), 7(d), 7(f), 8(b), and 8(d)). The values of the kinetic constants and parameters are listed in Table 2. According to the extremely high values of R^2, the model agrees with the experimental data very well. k_n is regarded as the adsorption rate constant of the kinetic model. The highest value of k_n was obtained at 200 ml/min of gas flow rate under the conditions of 5 mol % of CO_2/N_2, 0.025 g/ml of the sorbent fraction and at 20°C and 101.3 kPa, using CPEI-3. However, the equilibrium adsorption capacity (q_e) did not increase with the increase of the gas flow rate. That is because the increase of the gas flow rate will reduce the gas-liquid contact time [66], resulting in the reduced n values.

The parameters n and m reflect the effect of the driving force and the diffusion resistance [44]. Based on the data listed in Table 2, the values of m are higher compared to the values of n indicating the diffusion resistance had a greater influence on the rate of CO_2 adsorption on CPEI sorbents. Within the temperature range of the study, the value of m and n reached the extremum, respectively, at 30°C under the conditions of 0.025 g/ml of the sorbent fraction, 5 mol % of CO_2/N_2, and 100 ml/min of the gas flow rate under 101.3 kPa, using CPEI-3. The CO_2 adsorption of CPEI in the SBCR probably occurs in three stages: first, dissolution of CO_2 in water; in the second stage, diffusion of CO_2 across the water film surrounding each sorbent; finally, the adsorption of CO_2 to the sorbent by reacting amines. When the adsorption temperature increased from 20 to 30°C, the m value dropped to the minimum, indicating the dissolution and the diffusion rate of CO_2 in the water of the slurry reached the maximum. When the adsorption temperature was increased over 30°C, the desorption rate of CO_2 from slurry become dominant increasing the value of m. On the other hand, the negative effect of high temperature on the thermodynamics of the exothermic reaction between CO_2 and the amines of sorbent also resulted in the reduced value of n.

The elevated value of m with the increase of sorbent fraction is due to the increase in slurry viscosity caused by a strong interaction between particles [67]. Increasing the CO_2 fraction can increase both the driving force n and the diffusion resistance m (Table 2). Therefore, the CO_2 capacity did not increase accordingly with the increase of CO_2 fraction. The value of n increases with the elevation of the PEI/GA ratio since the number of amines available for CO_2 adsorption increased.

3.5. Cyclic Adsorption/Desorption. Reusability of adsorbents determines the efficiency and feasibility of a CO_2 capture technology [68]. The practical industrial applications require that the sorbents do not simply have a high CO_2 adsorption working capacity but also are stable for long-term operation.

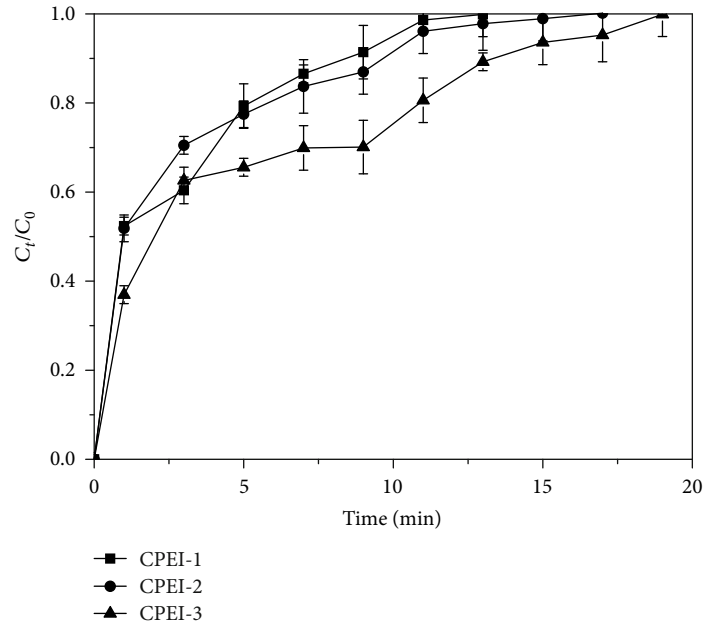

(a)

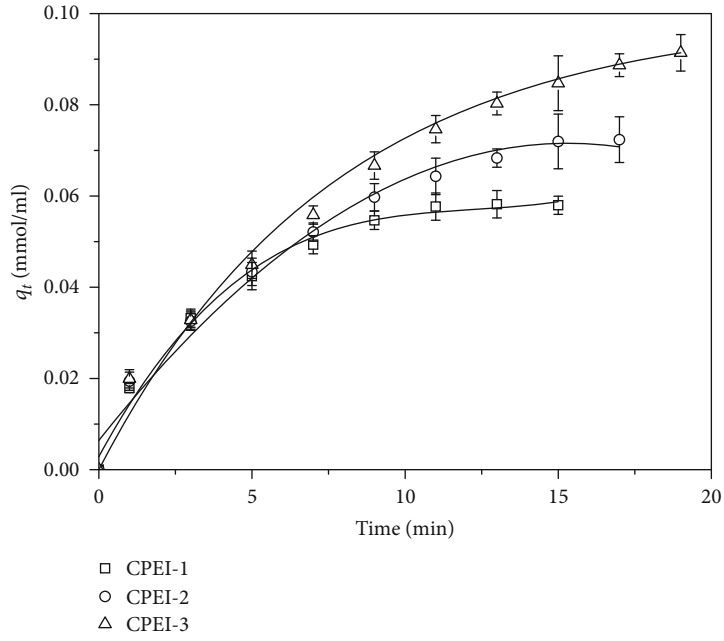

(b)

Figure 7: Continued.

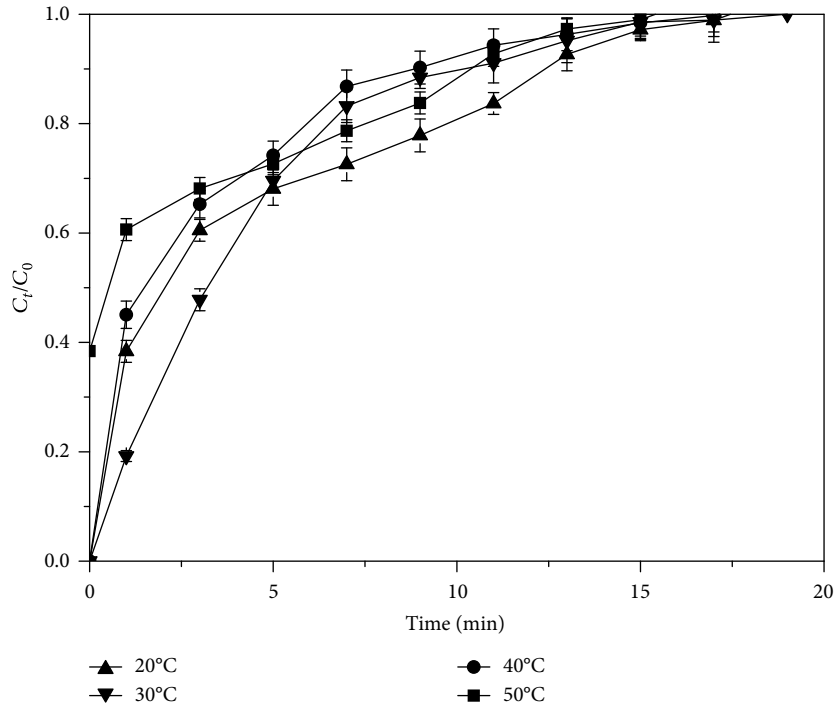

(c)

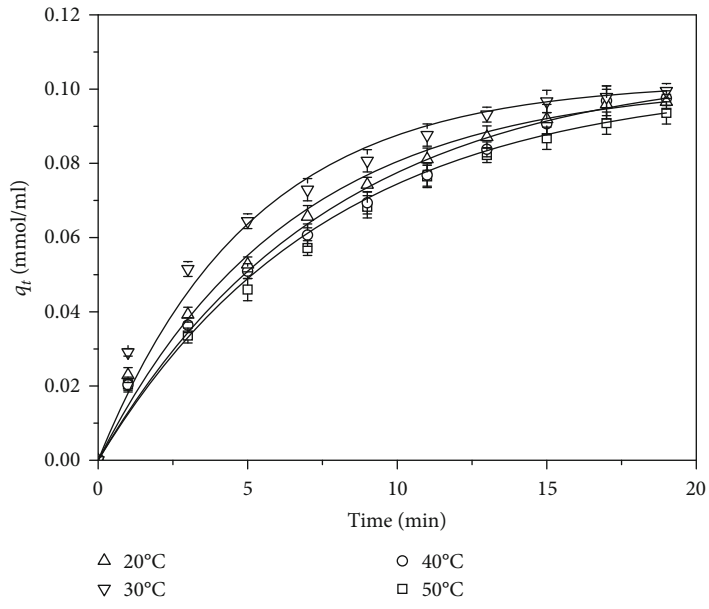

(d)

Figure 7: Continued.

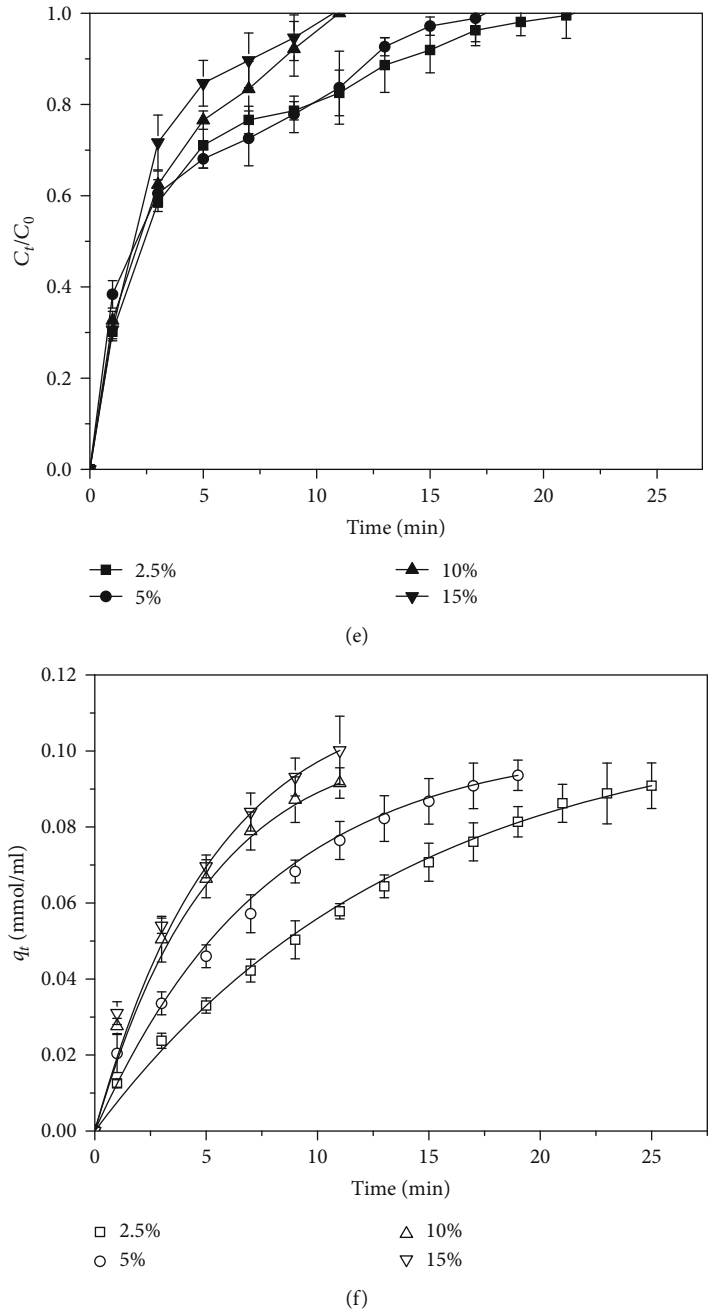

Figure 7: Breakthrough curves and CO_2 capture of slurry of CPEI-1, CPEI-2, and CPEI-3 (a, b), at different temperatures using CPEI-3 (c, d), various mol % of CO_2/N_2 mixture (e, f) using CPEI-3, under 101.3 kPa.

Ideally, CO_2 adsorbents should be regenerable, meaning that they should be able to undergo numerous adsorption/desorption cycles without noticeable loss of adsorption capacity. To study the multicycle behavior of CPEI sorbents in the SBCR for CO_2 adsorption, ten consecutive cycles of repeated adsorption/desorption operation were conducted under the conditions of 0.025 g/ml of the sorbent fraction, 5 mol % of CO_2/N_2, and 100 ml/min of the gas flow rate at 30°C and 101.3 kPa, using CPEI-3. The dynamic curves of the CO_2 capture in the SBCR in consecutive cycles of ten runs are displayed in Figure 9. After draining the water out of the reactor, the regeneration of CPEI-3 was accomplished by purging N_2 at 100°C until no CO_2 or water was detected in the exhaust gas. The results show that the CO_2 capacity of CPEI slurry decreased by about $1.5 \pm 0.5\%$ after ten cycles of operations.

The regenerability of CPEI-3 was also examined by the TGA method. The CPEI sorbents previously saturated with CO_2 were submitted to a temperature swing desorption of the adsorbed gas in the purified N_2 gas stream at 100°C for about 20 min. The sorbent was then used again for CO_2 adsorption on the same TGA setup. The repeated adsorption/desorption operation was performed for twenty cycles (Figure 10). The CO_2 capacity decreased by about 1% after

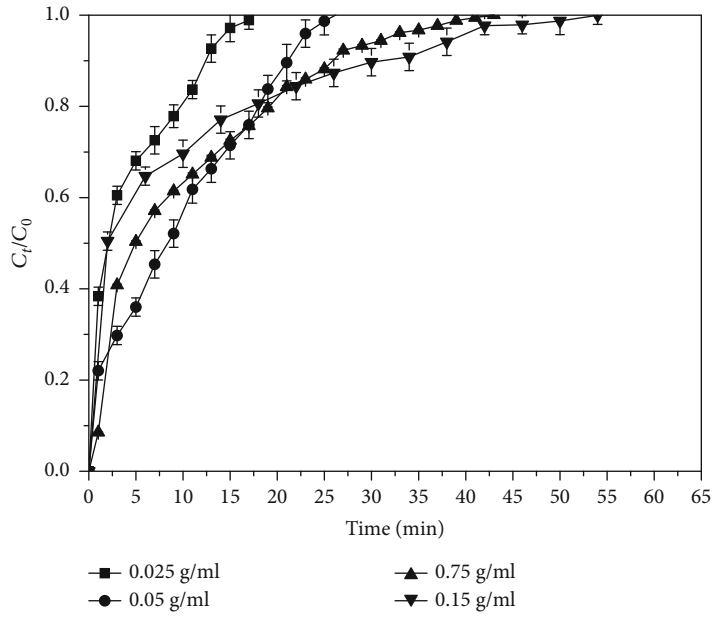

(a)

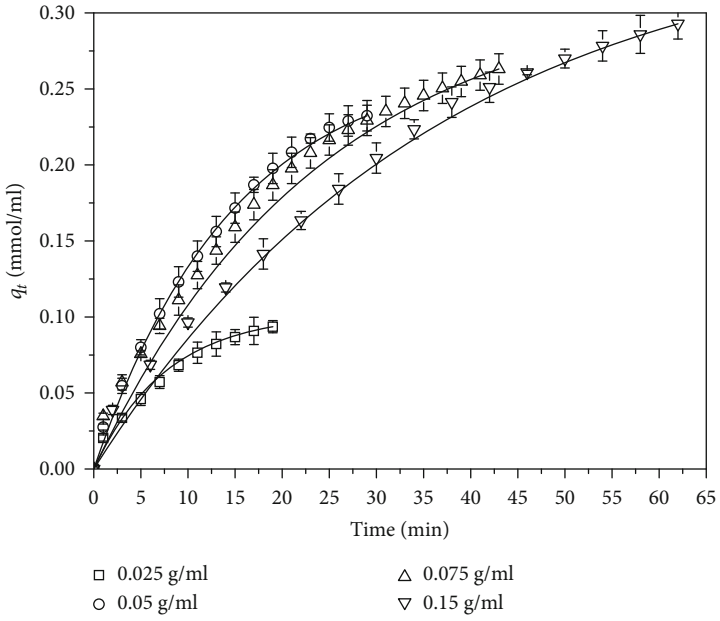

(b)

Figure 8: Continued.

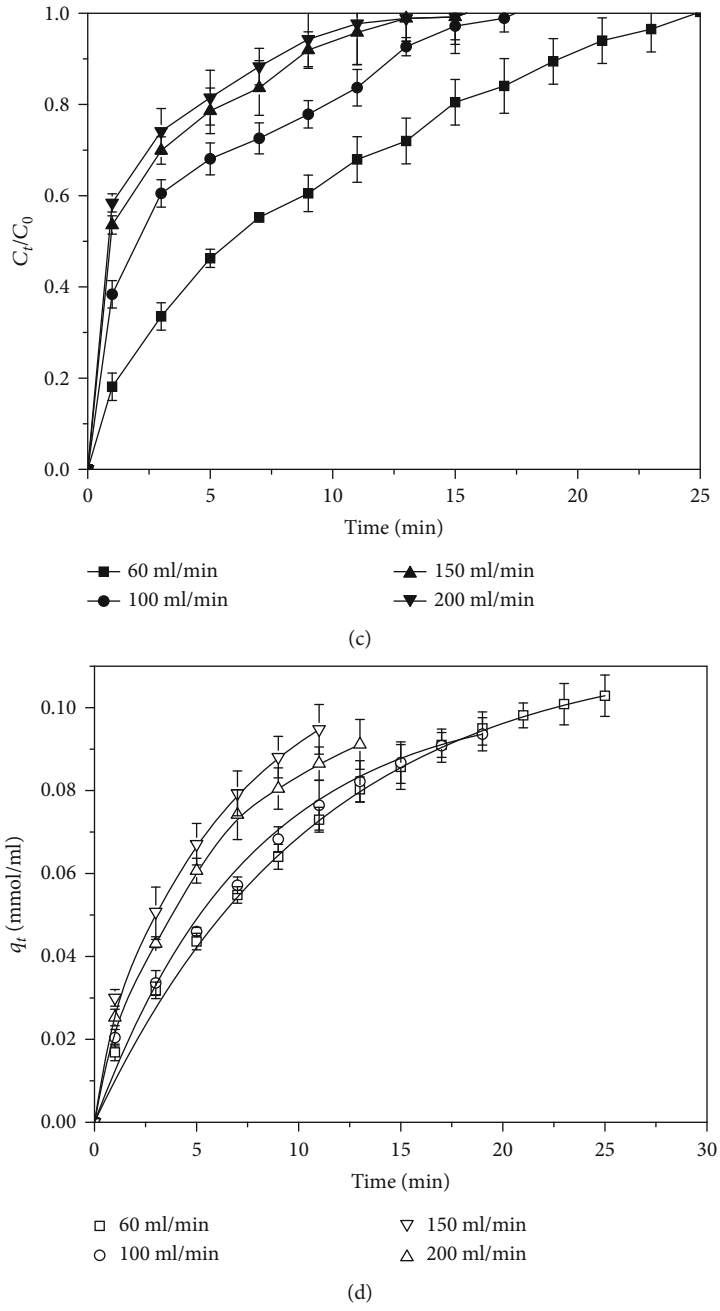

FIGURE 8: Breakthrough curves and CO_2 capacity of CPEI-3 in the SBCR at different sorbent fractions (a, b) or at various flow rates of CO_2/N_2 gas (c, d). The influence of sorbent fraction was evaluated under the conditions of 5 mol % CO_2/N_2 mixture, 100 ml/min of gas flow rate at 20°C and 101.3 kPa. The influences of gas flow rate were investigated under the conditions of 5 mol % CO_2/N_2 mixture, 0.025 g/ml of the sorbent fraction at 20°C and 101.3 kPa.

20 cycles of adsorption/desorption operation. Hence, CPEI sorbent exhibited good regenerability.

4. Conclusions

The CO_2 adsorption on the sorbent of CPEI was evaluated using an SBCR and under anhydrous condition by TGA. The CPEI-3 sorbent prepared at the PEI/GA ratio of 7 : 1 demonstrated the highest CO_2 adsorption capacity. The CO_2 capacity of the sorbent reached 4.92 mmol/g in the SBCR, which is 1.97 times higher than that obtained by TGA (2.5 mmol/g). The CO_2 adsorption kinetics of the CPEI slurry in the SBCR were well fitted by the fractional-order kinetic model. This indicates the CO_2 adsorption involved more than one reaction pathway. The modeling also demonstrated the diffusion resistance played the main role in the CO_2 adsorption by the CPEI sorbent. The CO_2 capacity decreased by about 1.5 ± 0.5% after 10 cycles of adsorption/-desorption in the SBCR. The promoting effect of H_2O on the CO_2 adsorption on the CPEI sorbent implies the potential

Table 2: Values of the kinetic model parameters.

	q_e (mmol/ml)	k_n (mmol^{1-m}/ml^{1-m} · min^n)	m	n	R^2
Temperature (°C)[†]					
20	0.0931	0.0358	0.648	0.335	0.9986
30	0.0998	0.0399	0.548	0.367	0.9993
40	0.0977	0.0219	0.627	0.278	0.9988
50	0.0932	0.0201	0.680	0.229	0.9969
Sorbent fraction (g/ml)[‡]					
0.025	0.0930	0.0353	0.651	0.339	0.9969
0.05	0.233	0.0371	0.702	0.355	0.9996
0.075	0.261	0.0398	0.737	0.375	0.9980
0.15	0.291	0.0369	0.766	0.297	0.9980
Gas flow rate (ml/min)[⁋]					
60	0.103	0.0243	0.718	0.306	0.9993
100	0.0966	0.0351	0.680	0.347	0.9969
150	0.091	0.0404	0.646	0.296	0.9987
200	0.0948	0.0437	0.563	0.254	0.9990
CO_2/N_2 fraction (mol%)[⊠]					
2.5	0.0912	0.0142	0.753	0.240	0.9991
5	0.0937	0.0352	0.681	0.339	0.9969
10	0.0947	0.0372	0.629	0.387	0.9996
15	0.0980	0.0386	0.555	0.153	0.9994
PEI/GA ratio[⸸]					
CPEI-1	0.0585	0.0301	0.699	0.234	0.9988
CPEI-2	0.0718	0.0327	0.679	0.272	0.9970
CPEI-3	0.0938	0.0358	0.648	0.351	0.9986

[†]Under the conditions of 0.025 g/ml of the sorbent fraction, 5 mol% of CO_2/N_2 and 100 ml/min of the gas flow rate using CPEI-3. [‡]Under the conditions of 5 mol% CO_2/N_2, 100 ml/min of the gas flow rate and at 20°C using CPEI-3. [⁋]Under the conditions of 5 mol% CO_2/N_2, 0.025 g/ml of the sorbent fraction and at 20°C using CPEI-3. [⊠]At 20°C, 0.025 g/ml of the sorbent fraction with the gas flow rate of 100 ml/min using CPEI-3. [⸸]Under the adsorption conditions of 0.025 g/ml of the sorbent fraction, 5 mol% of CO_2/N_2, and 100 ml/min of gas flow rate at 20°C.

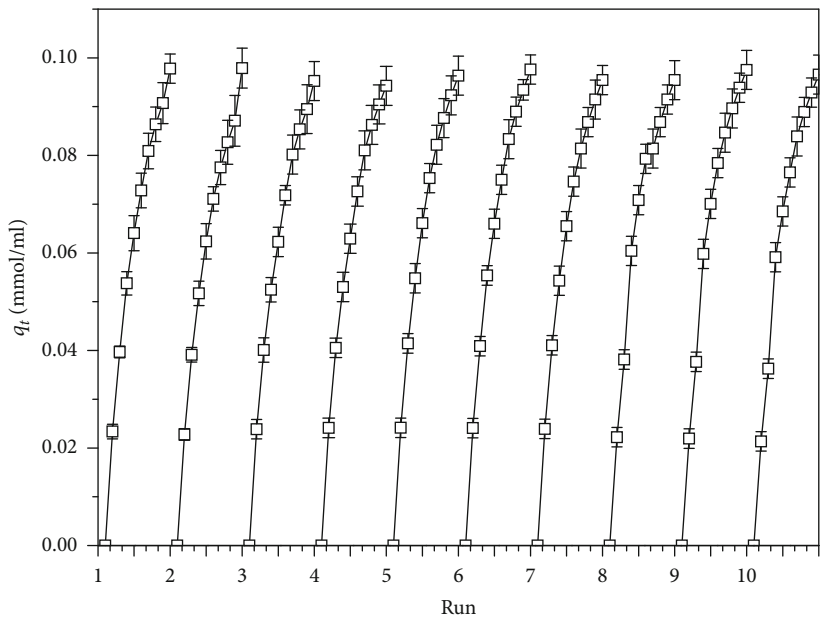

Figure 9: CO_2 capture of CPEI sorbent slurry in the SBCR during adsorption/desorption cycles under the conditions of 0.025 g/ml of the sorbent fraction, 5 mol % CO_2/N_2, 100 ml/min the gas flow rate at 30°C and 101.3 kPa using CPEI-3.

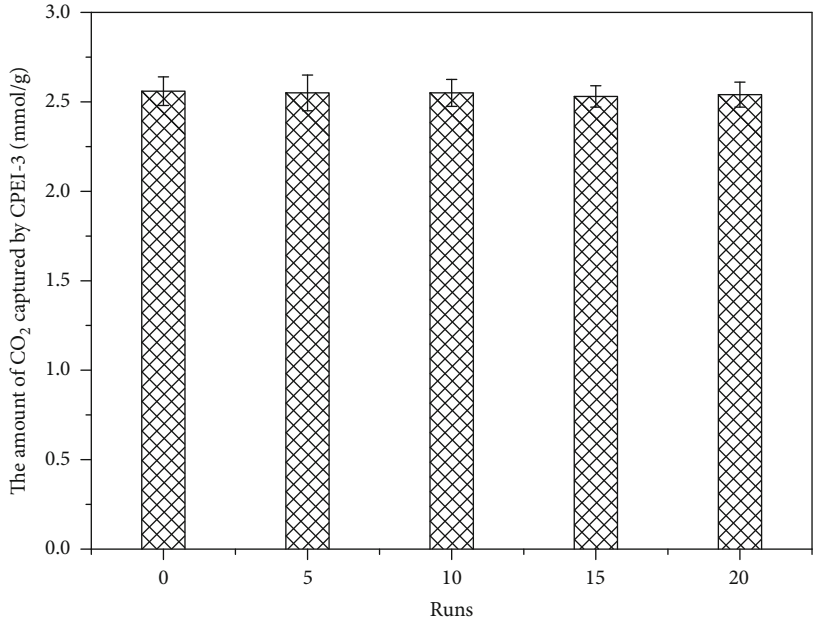

Figure 10: Reusability of the CPEI-3 sorbent for CO_2 capture determined by TGA. At the end of each run, the sorbent was regenerated by purging with N_2 at 100°C for about 20 min, until no CO_2 was detected in the exhaust gas.

application of the sorbent in the purification of the gas stream in the fermentation plant, the food factory, the thermal power station, or the submarine where water is available.

Data Availability

All data generated or analyzed during this study are included in this published article (and its supplementary information files).

Conflicts of Interest

The authors declared no potential conflicts of interest with respect to the research, authorship, and/or publication of this article.

Acknowledgments

The authors disclosed receipt of the following financial support for the research, authorship, and/or publication of this article: this work was supported by the Postgraduate Research and Practice Innovation Program of Jiangsu Province (SJCX18-0618).

Supplementary Materials

The supplementary material is available free of charge at https://SEM images of CPEI sorbent prepared at different ratio of PEI to GA (g : g) (word). *(Supplementary Materials)*

References

[1] G. Bertoni, C. Ciuchini, and R. Tappa, "Measurement of long-term average carbon dioxide concentrations using passive diffusion sampling," *Atmospheric Environment*, vol. 38, no. 11, pp. 1625–1630, 2004.

[2] K. Azuma, N. Kagi, U. Yanagi, and H. Osawa, "Effects of low-level inhalation exposure to carbon dioxide in indoor environments: a short review on human health and psychomotor performance," *Environment International*, vol. 121, pp. 51–56, 2018.

[3] J. T. James and A. Macatangay, "Carbon dioxide-our common enemy. NASA Technical Report No. JSC-CN-18669," NASA/-Johnson Space Center, Houston, TX, USA, 2009.

[4] X. Wang, X. Ma, V. Schwartz et al., "A solid molecular basket sorbent for CO_2 capture from gas streams with low CO_2 concentration under ambient conditions," *Physical Chemistry Chemical Physics*, vol. 14, no. 4, pp. 1485–1492, 2012.

[5] R. Serna-Guerrero and A. Sayari, "Modeling adsorption of CO_2 on amine-functionalized mesoporous silica. 2: kinetics and breakthrough curves," *Chemical Engineering Journal*, vol. 161, no. 1-2, pp. 182–190, 2010.

[6] A. Samanta and S. S. Bandyopadhyay, "Absorption of carbon dioxide into aqueous solutions of piperazine activated 2-amino-2-methyl-1-propanol," *Chemical Engineering Science*, vol. 64, no. 6, pp. 1185–1194, 2009.

[7] T. N. G. Borhani, M. Afkhamipour, A. Azarpour, V. Akbari, S. H. Emadi, and Z. A. Manan, "Modeling study on CO_2 and H_2S simultaneous removal using MDEA solution," *Journal of Industrial and Engineering Chemistry*, vol. 34, pp. 344–355, 2016.

[8] A. Goli, A. Shamiri, A. Talaiekhozani, N. Eshtiaghi, N. Aghamohammadi, and M. K. Aroua, "An overview of biological processes and their potential for CO_2 capture," *Journal of Environmental Management*, vol. 183, pp. 41–58, 2016.

[9] A. Kundu, J. K. Basu, and G. Das, "A novel gas–liquid contactor for chemisorption of CO_2," *Separation and Purification Technology*, vol. 94, pp. 115–123, 2012.

[10] Y. Peng, B. Zhao, and L. Li, "Advance in post-combustion CO_2 capture with alkaline solution: a brief review," *Energy Procedia*, vol. 14, pp. 1515–1522, 2012.

[11] M. L. Gray, Y. Soong, K. J. Champagne et al., "Improved immobilized carbon dioxide capture sorbents," *Fuel Processing Technology*, vol. 86, no. 14-15, pp. 1449–1455, 2005.

[12] E. S. Sanz-Pérez, C. R. Murdock, S. A. Didas, and C. W. Jones, "Direct capture of CO_2 from ambient air," *Chemical Reviews*, vol. 116, no. 19, pp. 11840–11876, 2016.

[13] X. Shen, H. du, R. H. Mullins, and R. R. Kommalapati, "Polyethylenimine applications in carbon dioxide capture and separation: from theoretical study to experimental work," *Energy Technology*, vol. 5, no. 6, pp. 822–833, 2017.

[14] A. Goeppert, M. Czaun, R. B. May, G. K. S. Prakash, G. A. Olah, and S. R. Narayanan, "Carbon dioxide capture from the air using a polyamine based regenerable solid adsorbent," *Journal of the American Chemical Society*, vol. 133, no. 50, pp. 20164–20167, 2011.

[15] A. Samanta, A. Zhao, G. K. Shimizu, P. Sarkar, and R. Gupta, "Post-combustion CO_2 capture using solid sorbents: a review," *Industrial & Engineering Chemistry Research*, vol. 51, no. 4, pp. 1438–1463, 2011.

[16] L. Keller, B. Ohs, L. Abduly, and M. Wessling, "Carbon nanotube silica composite hollow fibers impregnated with polyethylenimine for CO_2 capture," *Chemical Engineering Journal*, vol. 359, pp. 476–484, 2019.

[17] F. S. Taheri, A. Ghaemi, A. Maleki, and S. Shahhosseini, "High CO_2 adsorption on amine-functionalized improved mesoporous silica nanotube as an eco-friendly nanocomposite," *Energy & Fuels*, vol. 33, no. 6, pp. 5384–5397, 2019.

[18] R. P. Wijesiri, G. P. Knowles, H. Yeasmin, A. F. A. Hoadley, and A. L. Chaffee, "CO_2 capture from air using pelletized polyethylenimine impregnated MCF silica," *Industrial & Engineering Chemistry Research*, vol. 58, no. 8, pp. 3293–3303, 2019.

[19] H. Yang, W. Li, J. Liu, Y. Sun, and W. Liu, "Polyethylenimine-impregnated resins: the effect of support structures on selective adsorption for CO_2 from simulated biogas," *Chemical Engineering Journal*, vol. 355, pp. 822–829, 2019.

[20] A. Goeppert, M. Czaun, G. K. Surya Prakash, and G. A. Olah, "Air as the renewable carbon source of the future: an overview of CO_2 capture from the atmosphere," *Energy & Environmental Science*, vol. 5, no. 7, pp. 7833–7853, 2012.

[21] Q. Ye, J. Jiang, C. Wang, Y. Liu, H. Pan, and Y. Shi, "Adsorption of low-concentration carbon dioxide on amine-modified carbon nanotubes at ambient temperature," *Energy & Fuels*, vol. 26, no. 4, pp. 2497–2504, 2012.

[22] M. J. Schladt, T. P. Filburn, and J. J. Helble, "Supported amine sorbents under temperature swing absorption for CO_2 and moisture capture," *Industrial & Engineering Chemistry Research*, vol. 46, no. 5, pp. 1590–1597, 2007.

[23] W. Jung, J. Park, and K. S. Lee, "Kinetic modeling of CO_2 adsorption on an amine- functionalized solid sorbent," *Chemical Engineering Science*, vol. 177, no. 23, pp. 122–131, 2018.

[24] N. Rao, M. Wang, Z. Shang, Y. Hou, G. Fan, and J. Li, "CO_2 adsorption by amine-functionalized MCM-41: a comparison between impregnation and grafting modification methods," *Energy & Fuels*, vol. 32, no. 1, pp. 670–677, 2018.

[25] W. Si, S. Ye, D. Zhang et al., "Kinetics and mechanism of low-concentration CO_2 adsorption on solid amine in a humid confined space," *The Canadian Journal of Chemical Engineering*, vol. 97, no. 3, pp. 697–701, 2019.

[26] D. Wang, X. Wang, and C. Song, "Comparative study of molecular basket sorbents consisting of polyallylamine and polyethylenimine functionalized SBA-15 for CO_2 capture from flue gas," *ChemPhysChem*, vol. 18, no. 22, pp. 3163–3173, 2017.

[27] C. Knöfel, J. Descarpentries, A. Benzaouia et al., "Functionalised micro-/mesoporous silica for the adsorption of carbon dioxide," *Microporous and Mesoporous Materials*, vol. 99, no. 1-2, pp. 79–85, 2007.

[28] P. Li and F. H. Tezel, "Pure and binary adsorption equilibria of carbon dioxide and nitrogen on silicalite," *Journal of Chemical & Engineering Data*, vol. 53, no. 11, pp. 2479–2487, 2008.

[29] L. A. Darunte, A. D. Oetomo, K. S. Walton, D. S. Sholl, and C. W. Jones, "Direct air capture of CO_2 using amine functionalized MIL-101(Cr)," *ACS Sustainable Chemistry & Engineering*, vol. 4, no. 10, pp. 5761–5768, 2016.

[30] N. N. Linneen, R. Pfeffer, and Y. S. Lin, "CO_2 adsorption performance for amine grafted particulate silica aerogels," *Chemical Engineering Journal*, vol. 254, pp. 190–197, 2014.

[31] L. Wang and R. T. Yang, "Increasing selective CO_2 adsorption on amine-grafted SBA-15 by increasing silanol density," *The Journal of Physical Chemistry C*, vol. 115, no. 43, pp. 21264–21272, 2011.

[32] C.-H. Yu, C.-H. Huang, and C.-S. Tan, "A review of CO_2 capture by absorption and adsorption," *Aerosol and Air Quality Research*, vol. 12, no. 5, pp. 745–769, 2012.

[33] H.-B. Wang, P. G. Jessop, and G. Liu, "Support-free porous polyamine particles for CO_2 capture," *ACS Macro Letters*, vol. 1, no. 8, pp. 944–948, 2012.

[34] C.-J. Yoo, P. Narayanan, and C. W. Jones, "Self-supported branched poly(ethyleneimine) materials for CO_2 adsorption from simulated flue gas," *Journal of Materials Chemistry A*, vol. 7, no. 33, pp. 19513–19521, 2019.

[35] K.-S. Hwang, H.-Y. Park, J.-H. Kim, and J. Y. Lee, "Fully organic CO_2 absorbent obtained by a Schiff base reaction between branched poly(ethyleneimine) and glutaraldehyde," *Korean Journal of Chemical Engineering*, vol. 35, no. 3, pp. 798–804, 2018.

[36] L. B. Hamdy, R. J. Wakeham, M. Taddei, A. R. Barron, and E. Andreoli, "Epoxy cross-linked polyamine CO_2 sorbents enhanced via hydrophobic functionalization," *Chemistry of Materials*, vol. 31, no. 13, pp. 4673–4684, 2019.

[37] L. Cheng, T. Li, T. C. Keener, and J. Y. Lee, "A mass transfer model of absorption of carbon dioxide in a bubble column reactor by using magnesium hydroxide slurry," *International Journal of Greenhouse Gas Control*, vol. 17, pp. 240–249, 2013.

[38] K. S. Jung, T. C. Keener, V. C. Green, and S. J. Khang, "CO_2 absorption study in a bubble column reactor with Mg (OH) $_2$," *International Journal of Environmental Technology and Management*, vol. 4, no. 1/2, pp. 116–136, 2004.

[39] E. Sada, H. Kumazawa, and C. H. Lee, "Chemical absorption in a bubble column loading concentrated slurry," *Chemical Engineering Science*, vol. 38, no. 12, pp. 2047–2051, 1983.

[40] P. Mena, A. Ferreira, J. A. Teixeira, and F. Rocha, "Effect of some solid properties on gas–liquid mass transfer in a bubble column," *Chemical Engineering and Processing: Process Intensification*, vol. 50, no. 2, pp. 181–188, 2011.

[41] W. Wang, Q. Zeng, M. Li, W. Zheng, D. Christianson, and J. Economy, "Adsorptive removal of carbon dioxide using polyethyleneimine loaded glass fiber in a fixed bed," *Colloids*

and Surfaces A: Physicochemical and Engineering Aspects, vol. 481, pp. 117–124, 2015.

[42] A. L. Yaumi, M. Z. A. Bakar, and B. H. Hameed, "Melamine-nitrogenated mesoporous activated carbon derived from rice husk for carbon dioxide adsorption in fixed-bed," *Energy*, vol. 155, pp. 46–55, 2018.

[43] H. Thakkar, S. Eastman, A. Hajari, A. A. Rownaghi, J. C. Knox, and F. Rezaei, "3D-printed zeolite monoliths for CO_2 removal from enclosed environments," *ACS Applied Materials & Interfaces*, vol. 8, no. 41, pp. 27753–27761, 2016.

[44] A. Heydari-Gorji and A. Sayari, "CO_2 capture on polyethylenimine-impregnated hydrophobic mesoporous silica: experimental and kinetic modeling," *Chemical Engineering Journal*, vol. 173, no. 1, pp. 72–79, 2011.

[45] A. R. Cestari, E. F. S. Vieira, G. S. Vieira, and L. E. Almeida, "The removal of anionic dyes from aqueous solutions in the presence of anionic surfactant using aminopropylsilica—a kinetic study," *Journal of Hazardous Materials*, vol. 138, no. 1, pp. 133–141, 2006.

[46] J. L. Cohen, S. Schubert, P. R. Wich et al., "Acid-degradable cationic dextran particles for the delivery of siRNA therapeutics," *Bioconjugate Chemistry*, vol. 22, no. 6, pp. 1056–1065, 2011.

[47] S. Kakabakos, P. Tyllianakis, G. Evangelatos, and D. Ithakissios, "Colorimetric determination of reactive solid-supported primary and secondary amino groups," *Biomaterials*, vol. 15, no. 4, pp. 289–297, 1994.

[48] K. Dušek, M. Bleha, and S. Luňák, "Curing of epoxide resins: model reactions of curing with amines," *Journal of Polymer Science: Polymer Chemistry Edition*, vol. 15, no. 10, pp. 2393–2400, 1977.

[49] G. Socrates, *Infrared and Raman Characteristic Group Frequencies: Tables and Charts*, John Wiley & Sons, 2004.

[50] X. Yang, Q. Zhang, Y. Wang et al., "Self-aggregated nanoparticles from methoxy poly(ethylene glycol)-modified chitosan: synthesis; characterization; aggregation and methotrexate release in vitro," *Colloids and Surfaces B: Biointerfaces*, vol. 61, no. 2, pp. 125–131, 2008.

[51] I. Migneault, C. Dartiguenave, M. J. Bertrand, and K. C. Waldron, "Glutaraldehyde: behavior in aqueous solution, reaction with proteins, and application to enzyme crosslinking," *BioTechniques*, vol. 37, no. 5, pp. 790–802, 2004.

[52] M. Caplow, "Kinetics of carbamate formation and breakdown," *Journal of the American Chemical Society*, vol. 90, no. 24, pp. 6795–6803, 1968.

[53] S. A. Didas, M. A. Sakwa-Novak, G. S. Foo, C. Sievers, and C. W. Jones, "Effect of amine surface coverage on the co-adsorption of CO_2 and water: spectral deconvolution of adsorbed species," *The Journal of Physical Chemistry Letters*, vol. 5, no. 23, pp. 4194–4200, 2014.

[54] Z.-Z. Yang, L.-N. He, Y.-N. Zhao, B. Li, and B. Yu, "CO_2 capture and activation by superbase/polyethylene glycol and its subsequent conversion," *Energy & Environmental Science*, vol. 4, no. 10, pp. 3971–3975, 2011.

[55] T. L. Donaldson and Y. N. Nguyen, "Carbon dioxide reaction kinetics and transport in aqueous amine membranes," *Industrial & Engineering Chemistry Fundamentals*, vol. 19, no. 3, pp. 260–266, 1980.

[56] W.-C. Yu, G. Astarita, and D. W. Savage, "Kinetics of carbon dioxide absorption in solutions of methyldiethanolamine," *Chemical Engineering Science*, vol. 40, no. 8, pp. 1585–1590, 1985.

[57] F. A. Chowdhury, H. Yamada, T. Higashii, K. Goto, and M. Onoda, "CO_2 capture by tertiary amine absorbents: a performance comparison study," *Industrial & Engineering Chemistry Research*, vol. 52, no. 24, pp. 8323–8331, 2013.

[58] W. Jiang, X. Luo, H. Gao et al., "A comparative kinetics study of CO_2 absorption into aqueous DEEA/MEA and DMEA/-MEA blended solutions," *AICHE Journal*, vol. 64, no. 4, pp. 1350–1358, 2018.

[59] X. Wang and C. Song, "Temperature-programmed desorption of CO_2 from polyethylenimine-loaded SBA-15 as molecular basket sorbents," *Catalysis Today*, vol. 194, no. 1, pp. 44–52, 2012.

[60] W. Wang, J. Xiao, X. Wei, J. Ding, X. Wang, and C. Song, "Development of a new clay supported polyethylenimine composite for CO_2 capture," *Applied Energy*, vol. 113, pp. 334–341, 2014.

[61] C. Chen, W.-J. Son, K.-S. You, J. W. Ahn, and W. S. Ahn, "Carbon dioxide capture using amine-impregnated HMS having textural mesoporosity," *Chemical Engineering Journal*, vol. 161, no. 1-2, pp. 46–52, 2010.

[62] E. R. Monazam, J. Spenik, and L. J. Shadle, "Fluid bed adsorption of carbon dioxide on immobilized polyethylenimine (PEI): kinetic analysis and breakthrough behavior," *Chemical Engineering Journal*, vol. 223, pp. 795–805, 2013.

[63] X. Xu, C. Song, J. M. Andrésen, B. G. Miller, and A. W. Scaroni, "Preparation and characterization of novel CO_2 "molecular basket" adsorbents based on polymer-modified mesoporous molecular sieve MCM-41," *Microporous and Mesoporous Materials*, vol. 62, no. 1-2, pp. 29–45, 2003.

[64] Y. Yoshida, T. Katsumoto, S. Taniguchi, A. Shimosaka, Y. Shirakawa, and J. Hidaka, "Prediction of viscosity of slurry suspended fine particles using coupled DEM-DNS simulation," *Chemical Engineering Transactions*, vol. 32, pp. 2089–2094, 2013.

[65] D. Tiwari, H. Bhunia, and P. K. Bajpai, "Development of chemically activated N-enriched carbon adsorbents from urea-formaldehyde resin for CO_2 adsorption: kinetics, isotherm, and thermodynamics," *Journal of Environmental Management*, vol. 218, pp. 579–592, 2018.

[66] L. Tan, A. Shariff, K. Lau, and M. A. Bustam, "Factors affecting CO_2 absorption efficiency in packed column: a review," *Journal of Industrial and Engineering Chemistry*, vol. 18, no. 6, pp. 1874–1883, 2012.

[67] B. J. Konijn, O. B. J. Sanderink, and N. P. Kruyt, "Experimental study of the viscosity of suspensions: effect of solid fraction, particle size and suspending liquid," *Powder Technology*, vol. 266, pp. 61–69, 2014.

[68] T. C. Drage, K. M. Smith, A. Arenillas, and C. E. Snape, "Developing strategies for the regeneration of polyethylenimine based CO_2 adsorbents," *Energy Procedia*, vol. 1, no. 1, pp. 875–880, 2009.